JOURNAL OF MAGNETIC RESONANCE **134,** 67–71 (1998)
ARTICLE NO. MN981515

Low Frequency NMR Polarimeter for Hyperpolarized Gases

Brian T. Saam and Mark S. Conradi

Department of Physics, CB 1105, Washington University, St. Louis, Missouri 63130-4899

Received April 1, 1998

An inexpensive and self-contained apparatus for pulsed NMR at 30–250 kHz is described. The intended application is monitoring of the spin polarization of rare gas nuclei in a laser-polarizing apparatus in fields of order 30 G. In addition, the device provides a convenient method for following the polarization decay during storage and transport. Some of the features are a flexible pulse generator, splitting of transmitter RF cycles by the RF gate, a *Q* switch, and a wide range of receiver gains.

INTRODUCTION

In recent years, laser-driven techniques for producing high nuclear spin polarizations (1–40%) in rare gases have become widespread. These hyperpolarized gases have found numerous applications in fields as varied as neutron-beam physics (*1*) and biological MR imaging (*2*). Currently, MR imaging of the lung gas space (*3, 4*) and polarization transfer from rare gas nuclei to spins of greater analytical interest (e.g., protons or ^{13}C) (*5*) are both under rapid development.

Our laboratory uses depopulation optical pumping of dilute rubidium vapor at 795 nm which then slowly polarizes ^{3}He or ^{129}Xe nuclei by spin exchange (*6*). Approximately 0.4 L STP ^{3}He can be polarized to 40% in ~15 h. In trying to optimize this involved technique, diagnostic measurements are crucial. Thus, we observe the spectrum of the light transmitted through the polarizing cell, the nearby 780 nm fluorescence of the Rb, and the spatial distribution of light in the cell with an IR camera. But the most important diagnostic is the measurement closest to the overall goal—the nuclear spin polarization of the ^{3}He gas. We find *in situ* NMR polarization measurements using the device described herein to be invaluable and very convenient.

Several groups have low-field (the polarization is typically produced at 10–40 G) NMR apparatus for this purpose. Typically, the spectrometer is constructed of commercial instruments such as a frequency synthesizer, lock-in amplifiers, audio power amplifiers, and the like. By contrast, the present apparatus is a self-contained yet versatile pulsed NMR spectrometer for 30–250 kHz, requiring only an oscilloscope or other output recording device. The description here is offered because low-frequency NMR is so far from the experience of most NMR groups. The electronics described here (without oscilloscope and without 30 G Helmholtz coils) involve ≈$500 in parts.

OVERALL DESIGN

The spectrometer consists of four sections—the pulse generator, the transmitter, the duplexer and receiver, and the power supply.

The pulse generator is capable of generating up to a two-pulse sequence. Thus, one can generate spin echoes, though we have never done so. The pulse sequence may be initiated periodically (with adjustable period) or by a push-button (single shot). A muting delay is provided to gate the receiver off during probe ring-down. Likewise, a similar circuit is provided for driving a *Q* switch, to make ring-down more rapid.

The transmitter includes frequency generation, with frequencies of $1000/2n$ kHz ($n = 2$ to 16) available. For ^{3}He, 100 kHz is used; for ^{129}Xe, 31.25 kHz is used; both involve fields near 30 G. A digital gate and subsequent amplification produce transmitter outputs up to 20 V_{p-p}, more than sufficient for polarimetry. The gate handles the two half-cycles (+, −) of the carrier separately; this reduces the jitter in the nutation angle (compared to a simple digital gate) resulting from the small number of carrier cycles in a typical pulse. Synchronization of carrier phase and pulse timing is not necessary for our purposes.

The duplexer has a FET *Q* switch (*7*). The four-stage receiver is broadband (10–250 kHz), so a small amount of plug-in interstage filtering is used ($Q \approx 6$). The receiver was purposely designed with more gain than necessary for ^{3}He, particularly to accommodate its future use with ^{129}Xe, which has a smaller moment and is typically polarized at lower densities (*8*). Phase sensitive (lock-in, synchronous) detection at the carrier frequency (i.e., homodyne) is performed at a relatively high level, ~1 V. The receiving path finishes with postdetection gain and low-pass filtering. All of the gain stages except the first have switchable gain, to allow a wide dynamic range: even at 30 G, a 10 atm ^{3}He sample at 40% polarization generates ~10 mV signals in a tuned coil with a tip angle ≈5°.

1090-7807/98 $25.00

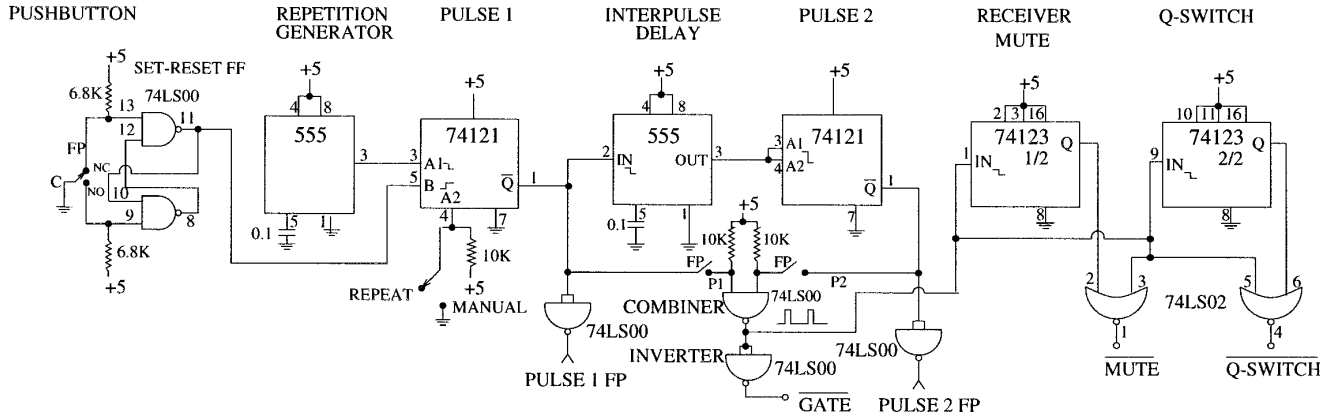

FIG. 1. Pulse generator circuit, allowing for up to two pulses per sequence. The combiner and switches allow one to choose which pulse (1, 2, or both) is sent to the transmitter. The two halves of the 74123 are pulse stretchers, for receiver muting and driving the *Q* switch into the low-*Q* state. None of the RC timing networks are shown. The designation FP means front panel location of the control.

CIRCUITRY

The descriptions of the circuitry will necessarily omit many details. For a full set of circuit diagrams, see the end of the article.

Power supply. The present design uses separate three-pin regulator chips on each of many boards. This provides the ultimate in power isolation between the several boards, but it is tedious. The supply proper is thus required to produce only positive and negative raw outputs of about 25 V, by full-wave rectification and capacitor-input filtering (*9*).

Pulse generator. The pulse generator is presented in Fig. 1. It is built in the main aluminum chassis (28 cm × 18 cm × 5 cm); like all the boards, it is constructed on perforated board with manual wire-wrap techniques. The pulse sequence may be initiated by a free-running (astable) 555 with period 0.1–100 s. Alternatively, a SPDT pushbutton (break-before-make) can initiate the sequence; the 74LS00 set–reset flip-flop is a standard debouncing circuit, sending only one pulse for each push of the switch. A two-position front panel switch selects between the free-run and single-shot modes.

The sequence initiation signal triggers the first pulse (74121 monostable, 10 μs–10 ms). This triggers an interpulse delay (555 monostable, 0.1–100 ms) which triggers the second pulse (another 74121). This sequence (1-delay-2) is always in place, but one can select (by switches) to use pulse 1, pulse 2, both pulses, or neither. The switches drive a 74LS00 combiner and inverter to produce the $\overline{\text{GATE}}$ pulse sent to the transmitter gate. To allow an oscilloscope or other data recorder to be triggered at a convenient time, the separate pulse 1 and pulse 2 outputs are available on the front panel, appropriately buffered.

The combined pulse signal is directed to a pair of pulse stretchers. These produce pulses that are longer than each gating pulse by an adjustable duration (from 10 μs to 10 ms). One, RECEIVER MUTE, gates the receiver off during the transmitter pulse and for a duration after (to allow for probe LC ringing). The other, *Q* SWITCH, generates the control signal for the *Q* switch (see later discussion).

All of the timing circuits (not shown in Fig. 1) use three-position switches to select a capacitor for decade selection; a variable resistor provides continuous coverage from ×1 to ×10.

Transmitter. The transmitter is built on two perforated boards inside the main chassis. The first board contains the 1 MHz crystal oscillator, $\div 2n$ circuitry, and the digital gate. The second board contains an analog switch (to improve on/off ratio) and the output stage. The boards are drawn together in Fig. 2.

The frequency generation circuitry is CMOS, for reduced power consumption. Four DIP switches on the circuit board select the frequency division ratio. The 74HCT161 counter is loaded with a preset count from the switches; on reaching 15 (binary 1111), the process is repeated. The D-type flip-flop, 74HCT74, gives a final factor of 2 division and produces an exactly 50% duty-cycle square wave. The $\bar{Q}$ output drives the receiver's phase-sensitive detector (see later discussion).

The *Q* output of 74HCT74 drives the digital gates, along with the $\overline{\text{GATE}}$ signal from the pulse generator. Basically, the output voltage is the average (by means of the 3.3 K resistors) of the two outputs at the 2.0 K resistors. With $\overline{\text{GATE}}$ high (unasserted), one output is high and the other is low. Thus, the junction of the 3.3 K resistors is essentially halfway between 0.4 and 4.5 V. When $\overline{\text{GATE}}$ becomes low (asserted), both outputs at the 2.0 K resistors are in-phase with each other at the selected carrier frequency. The resulting waveform, as shown in Fig. 2, results in less jitter in the nutation angle when working with pulses of few carrier cycles in duration. A pair of diodes improves the on/off ratio.

The entire first transmitter board can be turned off by removing the 5 V power to the board, by means of a front panel switch. This removes any possibility of the carrier leakage saturating the spins of the polarizing sample. Some of our cells

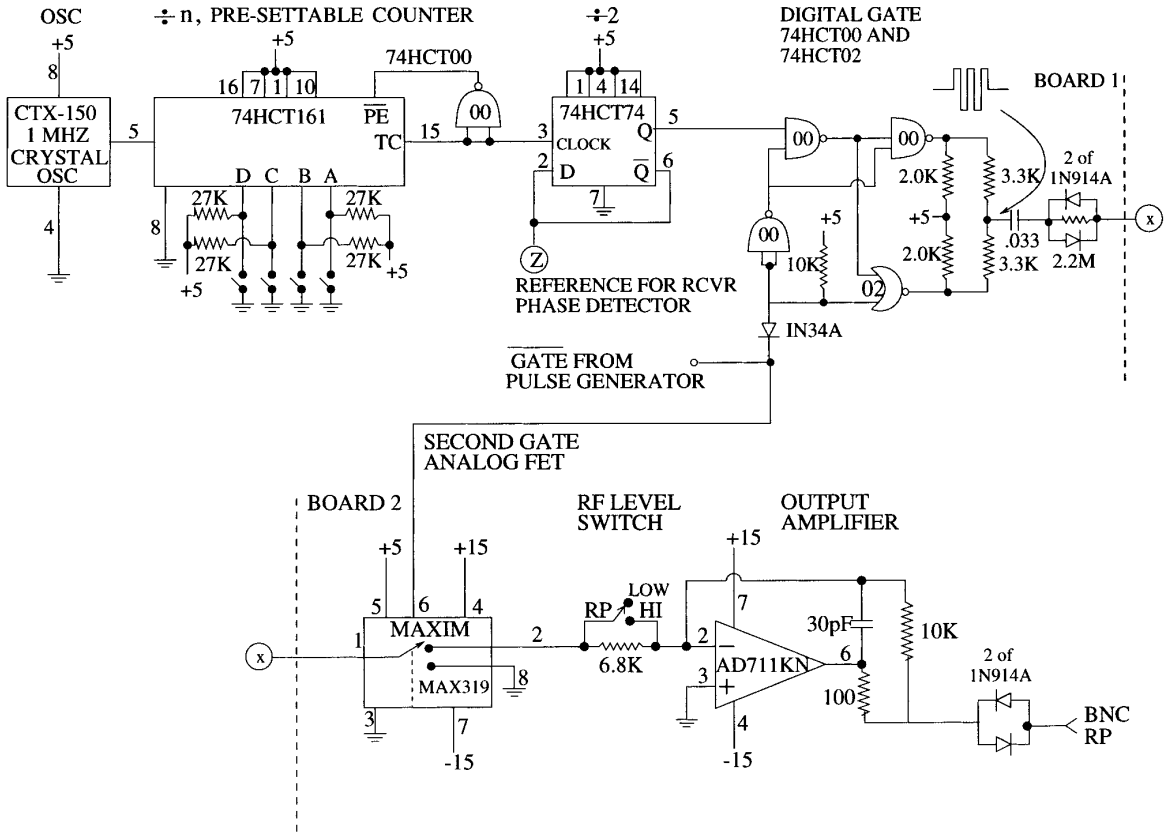

FIG. 2. Transmitter, consisting of CMOS oscillator and $\div 2n$ section, digital gate, analog FET IC gate, and output amplifier. For improved on/off ratio, the circuit is split into two boards. The power to board 1 can be removed during stand-by, to eliminate any possibility of saturating the spins. The RP designation means rear panel.

have $T_1 \sim 20-40$ h, so leakage is a concern. The 1N34A diode prevents the board from being powered(!) through the $\overline{\text{GATE}}$ line. We note that keeping the field off resonance may achieve the same goal, though shut-down of the oscillator power is foolproof.

The second board has an FET analog IC switch, run by the $\overline{\text{GATE}}$ line. This switch further improves the off-state rejection. The final amplifier, an Analog Devices AD711KN, is chosen for its fast output slewing. The output level of the pulse is switchable between 3 V_{p-p} and 20 V_{p-p} as measured by connecting the BNC output (Fig. 2) to a high-impedance oscilloscope instead of to the duplexer (T-R switch), which it normally feeds. The duplexer loads the transmitter output somewhat, so the voltage across the coil is lower and depends on how well the resonant circuit is tuned in transmit. Crossed diodes on the output are, again, to eliminate leakage in the pulse-off state (*10*).

Receiver and duplexer. A separate aluminum chassis (17 cm × 13 cm × 5 cm) holds the low-level circuitry—the duplexer and first three stages of receiver gain. This is done to improve on/off ratio, avoid oscillation of the high-gain receiver, and prevent the receiver from picking up spurious signals from the transmitter and pulse generator. Indeed, the present design has none of these problems.

The duplexer and receiver are displayed in Fig. 3. The tuning components are shown for 100 kHz (^{3}He at about 30 G) for use with a 900 μH NMR coil (single-coil, transmit–receive). The coil inductance L and the parallel capacitance C_T (50–1100 pF, 3-section variable) plus C_1 form a parallel resonant circuit of impedance $Q\omega L$. Here $Q \approx 90$ so the impedance level is near 50 kΩ. In receive, C_2 is just a coupling capacitor to the high input impedance of the first stage and the *N*-channel FET *Q* switch is biased off, with its gate at −15 V. The OP-27 preamplifier is good for a low impedance source, such as one might use at 30 kHz for ^{129}Xe. For higher input impedances, a FET-input amplifier will have better performance, because of its lower input noise current. In our ^{3}He application, the signals are quite strong and preamplifier noise is not an issue. Nevertheless, based on output noise measurements of this circuit, the equivalent input noise is on the order of the expected Johnson noise (*11*).

During transmit, the 1N914A diodes conduct, putting C_2 in parallel with C_T and C_1. The additional inductor L_2 offsets the increased capacitance. L_2 must not saturate under the maxi-

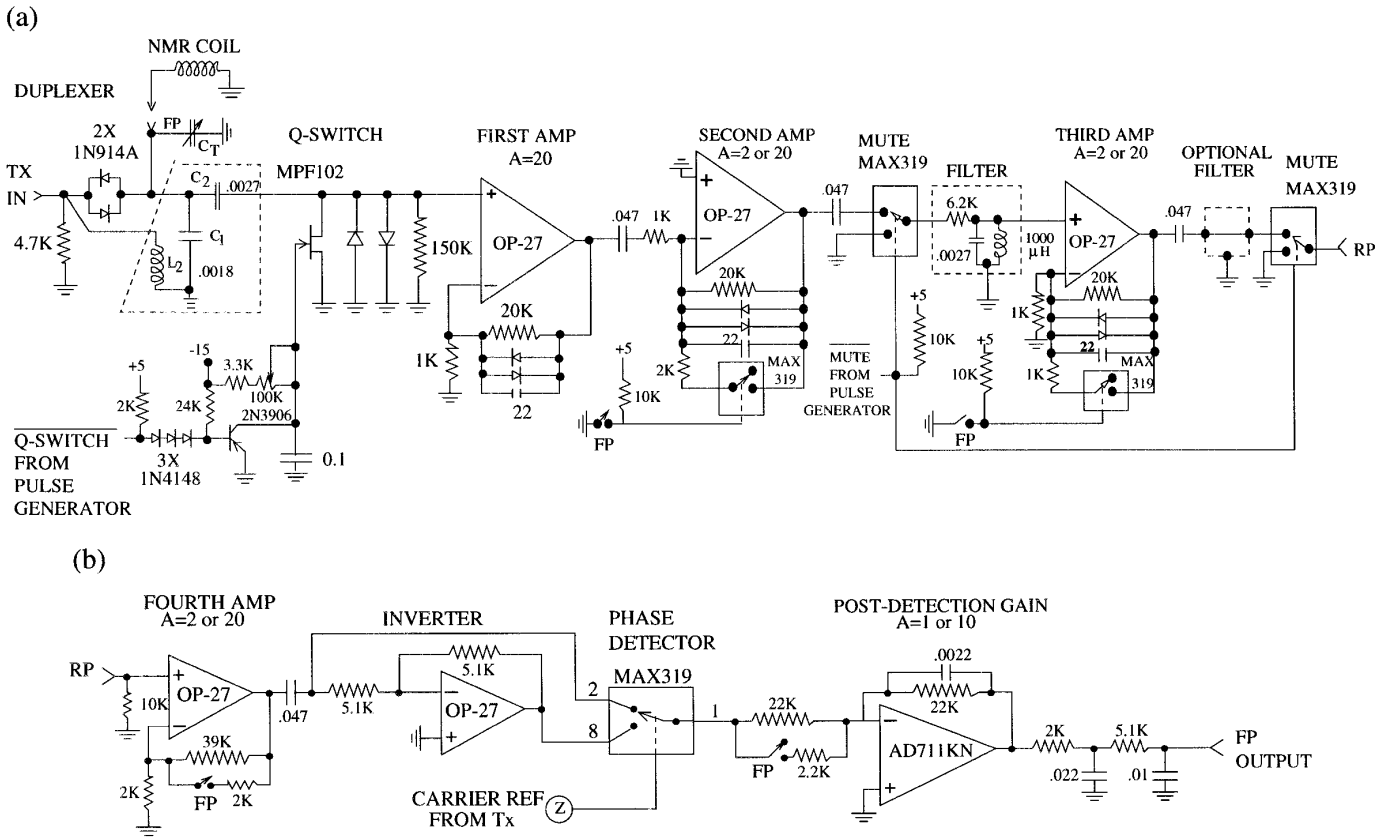

FIG. 3. (a) Duplexer (T-R switch), *Q* switch, and first three receiving amplifiers. The MAX319 are analog FET IC switches. Dashed lines surround plug-in, frequency-specific networks. (b) High-level section of receiver, including the phase-sensitive detector. All unmarked diode pairs are 1N914A.

mum transmitter output. The FET *Q*-switch remains on (≈300 Ω impedance) until the $\overline{Q\text{-SWITCH}}$ line returns high (unasserted *and* the 0.1 μF gate capacitor has recharged beyond the FET's pinch-off voltage. In the on-state, the *Q* of the input circuit is quite low, $Q \approx 2$, hastening the LC ring-down. The 1N4148 diodes driving the 2N3906 serve as a level shifter for the $\overline{Q\text{-SWITCH}}$ line.

The receiver's four stages of gain are AC-coupled. Each stage except the last is output-limited by crossed diodes in the feedback network, preventing overload of the following stage (*12*). Under high signal conditions, it is thus important to reduce the gain of stages 2 and 3 to avoid clipping by the diode limiters. In addition, the high-frequency response is rolled off by 22-pF capacitors. Except for the input stage, the gain of each stage is switchable between 2 and 20. On stages 2 and 3, the gain switching employs analog FET IC switches, Maxim MAX319. Thus, the front panel gain-control toggle switches carry only control voltages, reducing the chance of unwanted feedback. Two more MAX319 switches are used for receiver muting, driven by the pulse generator's $\overline{\text{MUTE}}$ line. A modest, $Q \approx 6$ filter is positioned between stages 2 and 3; another filter may be placed after stage 3. Both filters and the duplexer tuning components are plug-ins on 14 pin DIP component carriers.

The fourth receiver gain stage and all subsequent circuitry reside in the main chassis with the transmitter and power supply. The phase-sensitive detection (*13*) uses an analog FET switch to select between the signal (pin 2) and its invert (pin 8). The switch selection is driven by the square-wave carrier output from the 74HCT74 on the first transmitter board. Post-detection gain of ×1 or ×10 is followed by low-pass filtering with a roll-off starting near 3 kHz.

NMR COIL AND MAGNET

In our laboratory, optical pumping is performed in a ≈30 G field from a Helmholtz pair of 60 cm diameter and 30 cm separation. The coils have about 30 kg of copper wire and consume ≈115 W, dissipated to the air. The glass vessel containing Rb and ^{3}He with a small amount of N_2 fluorescence-quenching gas resides at the magnet center and rests on the NMR surface coil, inside the temperature-regulated oven. The ≈900 μH surface coil is 250 turns in 30 layers, with an average diameter of 1.4 cm and a height of 0.5 cm. The short coil is 0.3 cm from the polarizing vessel's lower surface. The coil is wound on a form made of Ultem 1000 (Gehr Plastics, Inc., Aston, PA), which can withstand the 160–200°C operating temperature of the oven. The wire used is 30 AWG copper

Litz wire (25 strands of individually insulated 44 AWG; Cooner Wire, Chatsworth, CA). The Q of the coil is 90, about three times that achieved with solid wire of the same gauge and geometry. The coil connects to the duplexer (Fig. 3) by ordinary coaxial cable; there are no tuning elements near the coil. We estimate that the NMR coil is sensitive to ~0.5% of the spins in the 3.5 cm diameter ×5 cm long vessel. The T_2^* of ^{3}He in this arrangement is about 60 ms.

PERFORMANCE

The low-field spectrometer described here has been in use for 5 months and gives a reliable measure of the relative polarization. Thus, the effects of changing laser power, oven temperature, or the position and elements of the laser optical train may be quantified by measuring the initial rate of polarization growth and the eventual steady-state polarization. We typically employ a single pulse of 650 μs with a 3 V_{p-p} amplitude. The receiver gain settings are typically ×2, ×2, ×20, and ×10 (postdetection). Often, the input circuit is intentionally detuned to reduce the signal.

One could easily simplify the design for a bare-bones polarization monitor. We would use a simpler, fixed frequency divider to generate 100 kHz. The pulse generator would have only a single pulse driven by the pushbutton. The mute timer and Q-switch timer would be controlled by circuit-board trimpots; simplification of the front panel would result. The receiver needs only three gain stages, of gains 20, 2 or 20, and 2 or 20. The postdetection gain should be fixed at 2. A large savings in effort could result from building the circuits on just two boards, each still in its own chassis. Each chassis would have its own power regulators, instead of the present design's separate regulators on each of the many boards.

Absolute polarimetry. To obtain the absolute level of polarization, $(u - d)/(u + d)$, where u and d are numbers of spins up and down, one needs to compare to a Boltzmann equilibrium signal. At 30 G, the equilibrium polarization of ^{3}He at room temperature is only 8×10^{-3} ppm. Thus, to compare 40% polarized gas with equilibrium gas would require an incredible dynamic range and much signal averaging. One could instead use water as the equilibrium signal, though the increase by ≈1000 in density still leaves the hyperpolarized and equilibrium signals far apart in magnitude.

Thus, we do absolute polarimetry at 64.7 MHz in a 2 T iron-core magnet. The signal can be compared to that of protons in glycerol (or water) at the same frequency. By working at high frequency the equilibrium polarization is made larger. Even at the high field, the gas signal may be 50 dB larger than the protons. To calculate the absolute gas (G) polarization P_G at fixed frequency f, one needs the Boltzmann proton (P) polarization $P_P \times hf/2kT$, the spin number densities N_G and N_P (the vessel shapes and sizes are the same), and the γ's (because the signal is proportional to both the nuclear magnetic moment and the tip angle, in the small tip-angle limit). Thus,

$$\frac{S_G}{S_P} = \frac{N_G}{N_P}\frac{P_G}{P_P}\frac{\gamma_G^2}{\gamma_P^2}.$$

The polarizations so calculated can then be transferred to calibrate the low-field spectrometer's output in terms of absolute polarization.

Full circuit diagrams can be obtained by writing to the authors.

ACKNOWLEDGMENTS

The authors gratefully acknowledge NSF support through Research Grant DMR-9705080. The assistance of Ryan Field and Catherine F. Clewett in constructing the spectrometer is appreciated.

REFERENCES

1. G. L. Greene, A. K. Thompson, and M. S. Dewey, *Nucl. Instrum. Methods A* **356,** 177 (1995).
2. B. Saam, *Nature Med.* **2,** 358 (1996).
3. J. P. Mugler, III, B. Driehuys, J. R. Brookeman, G. D. Cates, S. S. Berr, R. G. Bryant, T. M. Daniel, E. E. de Lange, J. H. Downs, C. J. Erickson, W. Happer, D. P. Hinton, N. F. Kassel, T. Maier, C. D. Phillips, B. T. Saam, K. L. Sauer, and M. E. Wagshul, *Magn. Reson. Med.* **37,** 809 (1997).
4. H.-U. Kauczor, M. Ebert, K.-F. Kreitner, H. Nilgens, R. Surkau, W. Heil, D. Hofmann, E. W. Otten, and M. Thelen, *J. Magn. Reson. Imag.* **7,** 538 (1997).
5. G. Navon, Y.-Q. Song, T. Rõõm, S. Appelt, R. E. Taylor, and A. Pines, *Science* **271,** 1848 (1996).
6. T. G. Walker and W. Happer, *Rev. Mod. Phys.* **69,** 629 (1997).
7. M. S. Conradi, *Rev. Sci. Instrum.* **48,** 359 (1977).
8. B. Driehuys, G. D. Cates, E. Miron, K. Sauer, D. K. Walter, and W. Happer, *Appl. Phys. Lett.* **69,** 1668 (1996).
9. H. V. Malmstadt, C. G. Enke, and S. R. Crouch, *in* "Electronics and Instrumentation for Scientists," p. 58, Benjamin/Cummings, Menlo Park, CA (1981).
10. E. Fukushima and S. B. W. Roeder, *in* "Experimental Pulse NMR: A Nuts and Bolts Approach," p. 388, Addison-Wesley, Reading, MA (1981).
11. J. C. Sprott, *in* "Introduction to Modern Electronics," p. 219, Wiley, New York (1981).
12. A. P. Malvino, *in* "Electronic Principles," 3rd ed., p. 549, McGraw-Hill, New York (1984).
13. P. Horowitz and W. Hill, *in* "The Art of Electronics," 2nd ed., p. 1031, Cambridge, Cambridge, UK (1989).